LA-UR-12-01000

Title:	Anisotropic and Pressure-Dependent Plasticity Modeling for Residual Stress Prediction
Author(s):	Michael B. Prime, W-13
Intended for:	Prime, M. B., 2013, "Anisotropic and Pressure-Dependent Plasticity Modeling for Residual Stress Prediction," Experimental and Applied Mechanics, Volume 4, Conf. Proc. of the Soc. for Experimental Mechanics Series, C. E. Ventura et al., eds., Springer New York, pp. 415-427

Anisotropic and Pressure-Dependent Plasticity Modeling for Residual Stress Prediction

Michael B. Prime (prime@lanl.gov)
Los Alamos National Laboratory, Los Alamos, NM 87545

ABSTRACT

In order to provide well characterized residual stress specimens, 10-mm thick, 60-mm diameter disks of 2024-T351 Aluminum were plastically indented by opposing 15-mm diameter indenters of hardened steel. The residual stresses in the disk specimen were measured using neutron diffraction, the contour method, and the slitting method. A finite element model of the indentation process was constructed, but matching the measured residual stresses proved unexpectedly challenging. An attempt was made to improve the agreement honestly (without any unjustified parameter changes) by improving the constitutive model for 2024. Cyclic stress-strain curves were measured in multiple directions in the source plate of 2024-T351 which showed plastic anisotropy on the order of 15% in the flow strength. Recent literature has also shown a pressure dependence in 2024-T351 which would increase the flow strength in the triaxial stress region under the indenter. Combining anisotropy, cyclic loading, and pressure dependence effects in Abaqus has significantly improved agreement with the data, but a completely accurate prediction remains elusive.

INTRODUCTION

Residual stresses play a significant role in many material failure processes like fatigue, fracture, and stress corrosion cracking [1,2]. Residual stresses are the stresses present in a part free from external load, and they are generated by virtually any manufacturing process. The subject of this study is indented-disk test specimens that were designed to provide a controlled distribution of residual stress [3] in order to develop and test methods for measuring residual stresses.

Accurate finite element modeling of the disk specimens has proven somewhat challenging. In previous work, accurate residual stress modeling for disks of 316L stainless steel was achieved only after cyclic testing and subsequent calibration of a combined hardening model to capture the Bauschinger effect [3]. In this paper, we explore accurate modeling for indented disks made of 2024-T351 Aluminum, which have proven even more challenging to model accurately.

EXPERIMENTAL

Disks were plastically compressed through the thickness by two cylindrical indenters of smaller diameter, see Figure 1. The disks of 2024-T351 aluminum were 60 mm in diameter and 10 mm thick. The indenter material used was A2 tool steel characterized by a high hardness (58 HRC) and a high yield stress (about 1300 MPa). The indentation was performed quasi-statically to a maximum load 99.6 kN and then unloaded. The residual stresses in the specimens were measured using neutron diffraction [4,5], the contour method [6-8], and the slitting method [9,10], with the measurement details on the 2024 specimen discussed in this paper reported elsewhere [3,11].

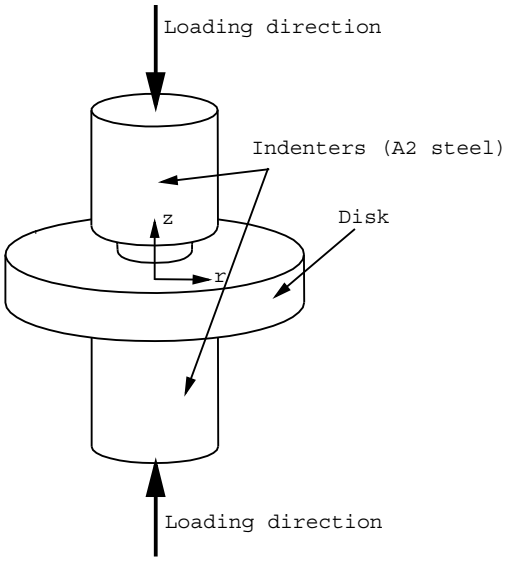

Figure 1 Indented disk residual stress specimens were made using 2024-T351 Aluminum

MODELING

The disk indentation process was modeled using ABAQUS version 6.11. For initial runs with isotropic plasticity models, a half-symmetry axi-symmetric model of the specimen, see Figure 2, was built using 15,000 four-node quadrilateral elements with reduced integration (CAX4R). Square elements 0.1 mm on a side gave a 50 x 300 mesh in the disk. The contact behavior between the indenter (master surface) and the disk (slave surface) was assumed frictionless because lubricant was used during the experimental test, and a surface-to-surface contact algorithm was used. A pressure load was applied to the top surface of the indenter to match the experimentally applied load. Figure 3 shows the $1/8^{th}$ symmetry, 3D mesh used for later simulations with anisotropic material models. 20 node brick elements with reduced integration (C3D20R) were used with elements approximately 0.5 mm on a side.

The indenter was modeled as elastic with Young's modulus of 204 GPa and Poisson's ratio of 0.3. For the Al 2024, the Young's modulus was 73.2 GPa and Poisson's ratio was 0.33. The plasticity model for the Al 2024 was varied during the study and is described below.

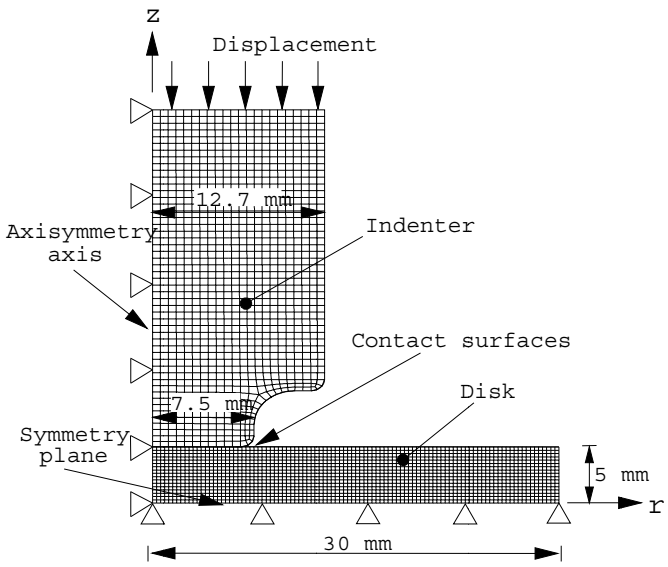

Figure 2 Axisymmetric finite element model

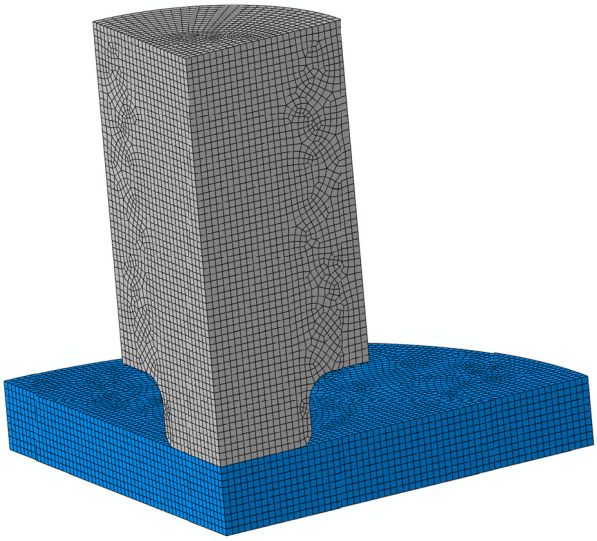

Figure 3 1/8th symmetry 3D finite element mesh for simulations with anisotropic material models

Model attempt using isotropic plasticity with combined hardening

Small compression samples were taken from the 12.7 mm thick Al 2024-T351 plate. The results showed modest plastic anisotropy, with the flow stress approximate same in the rolling and through-thickness directions of the Al 2024 plate, and about 10-15% lower in the transverse direction. Subsequently, specimens were extracted in the rolling and transverse directions of the plate and tested in compression-tension cyclic tests. The plate was too thick to extract such samples in the through-thickness direction. Figure 4, shows the data from the cyclic tests. Based on the nearly identical behavior in the loading-only compression tests, the through-thickness direction was assumed to have the same cyclic behavior as rolling direction.

Based on the experience with 316L specimens [3], a cyclic combined hardening model was carefully calibrated for the 2024 Al, see Figure 4. The resulting model prediction did not match the data very well; see Figure 5 and Figure 6. This anisotropy was ignored in this initial modeling because 15% errors in residual stress or strain would have been acceptable for this application. Note, however, that the ~15% plastic anisotropy in the flow stress has produced more than a factor of two difference in the residual radial strains, see Figure 5.

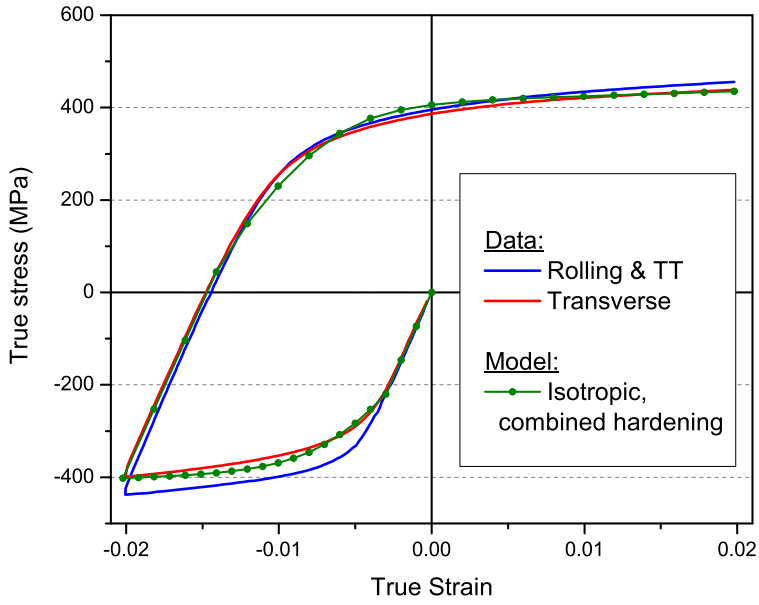

Figure 4 Isotropic plasticity, combined hardening cyclic stress-strain curves calibrated for 2024-T351 Aluminum alloy. The model fits the cyclic behavior but does not fit the anisotropy

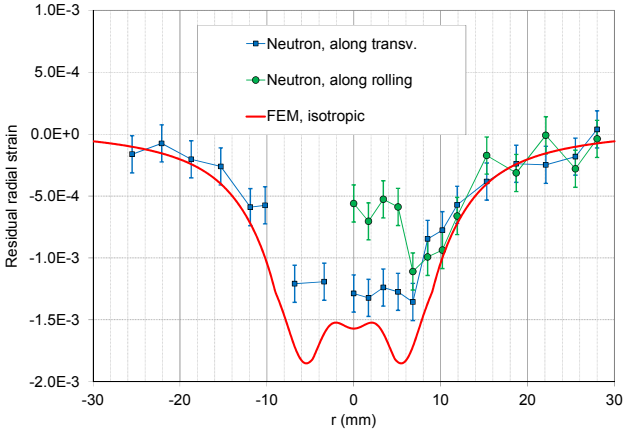

Figure 5 Residual elastic radial strains in 2024-T351 disk, model vs. data. Taken at mid-thickness along diameters of disk corresponding to rolling and transverse directions of plate material

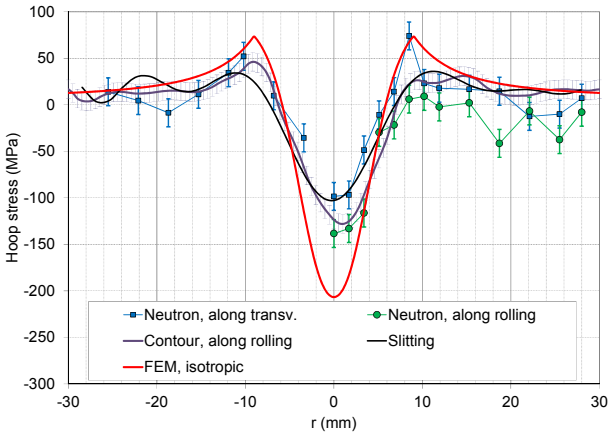

Figure 6 Residual Hoop Stress in 2024-T351 disk, models vs. data. Taken at mid-thickness along diameters of disk corresponding to rolling and transverse directions of plate material

Reverse Yielding

In ABAQUS, a combined hardening model cannot be used simultaneously with anisotropic plasticity, and clearly anisotropic plasticity is necessary to accurate model the stresses. A short study was performed to estimate the magnitude and importance of reverse yielding during unloading of the indenters on the disk. The constitutive data was fit using a kinematic hardening model. The model fit is shown in Figure 7. Such a model only allows for linear strain hardening, but does a reasonable job of fitting the loading portion of the data and conservatively estimates the reverse yielding.

A simulation of the indentation process with the kinematic hardening model showed no reverse plasticity during the unloading. Therefore, it should not be necessary to accurately model the cyclic behavior of the 2024 Al so long as premature reverse yielding is not predicted.

This simple model did not give a very good prediction of the residual stresses because of the inability of the model to fit the finer details in the loading portion of stress-strain curve, as shown in Figure 7. Although such details may seem minor, most of the disk only sees plastic strains of under 1%, which is where the fit is least accurate. Figure 8 shows the plastic strain in the disk after an indentation simulation. Except for a small stress concentration region near the edge of the indenter, the disk only sees plastic strains of less than 2%.

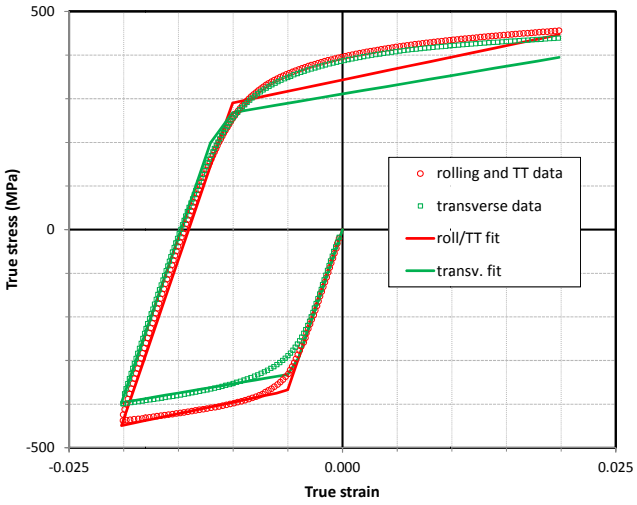

Figure 7 In order to check for reverse yielding, a anisotropic model with kinematic hardening was fit to the data

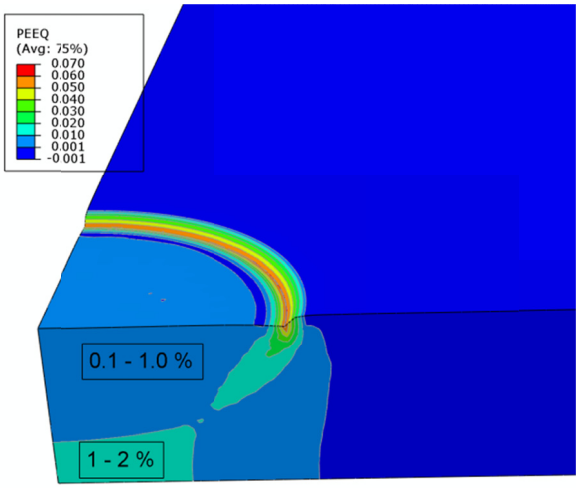

Figure 8 Equivalent plastic strains in the disk after the indentation simulation are mostly under 2%. (Deformation exaggerated by a factor of 10)

Anisotropic plasticity with isotropic hardening

Since it was no longer necessary to model the reverse plasticity, an anisotropic fit using isotropic hardening was used. Plastic anisotropy was modeled using Hill's potential function [12] in ABAQUS. Because the conversion of uniaxial stress-strain curves to effective-stress – effective-strain curves depends on the *R* ratios, an iterative process was used to fit the *R* ratios to the data. Figure 9 shows the fit for optimizing for the range of strains up to 1%, which gave an *R* of 1.16, or 16% anisotropy. This fit was applied in ABAQUS using the *POTENTIAL function to define the anisotropy and a tabular description of the stress-strain curve. Simple one element problems were used to verify that the implementation matched the calibration data of Figure 9.

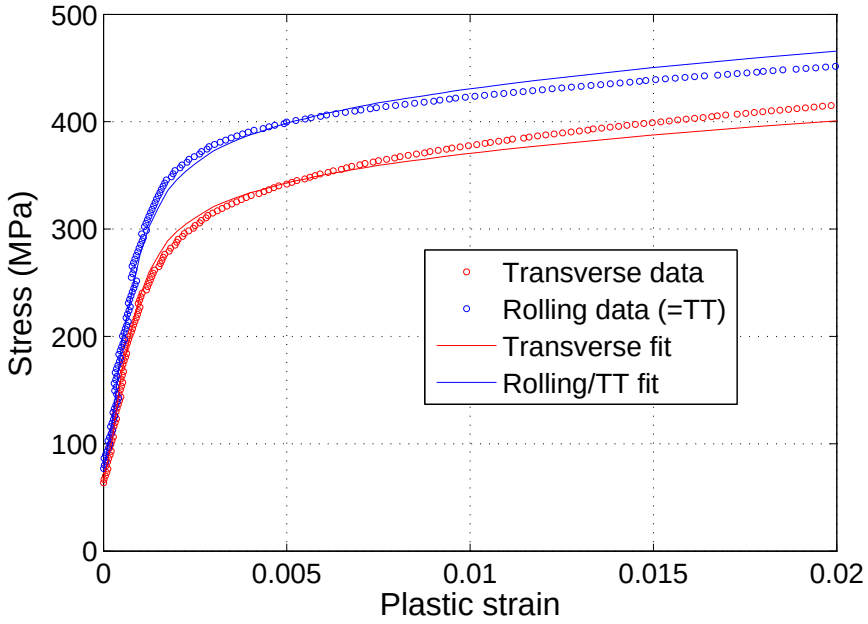

Figure 9 Anisotropic plasticity fit to data, optimized over range 0 – 1.0% plastic strain

The anisotropic model was used on the indentation simulation. The resulting residual strain and residual stress predictions are compared with data in Figure 10 and Figure 11. The model now shows the observed anisotropy in the results, but the overall magnitude is still incorrect.

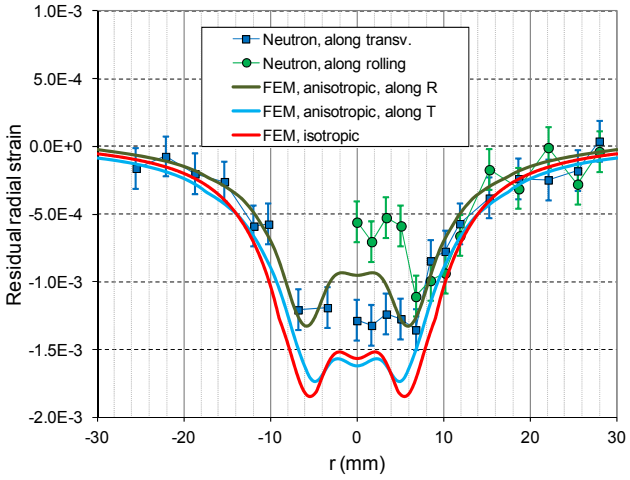

Figure 10 Residual elastic radial strains predicted with the anisotropic plasticity model, versus data

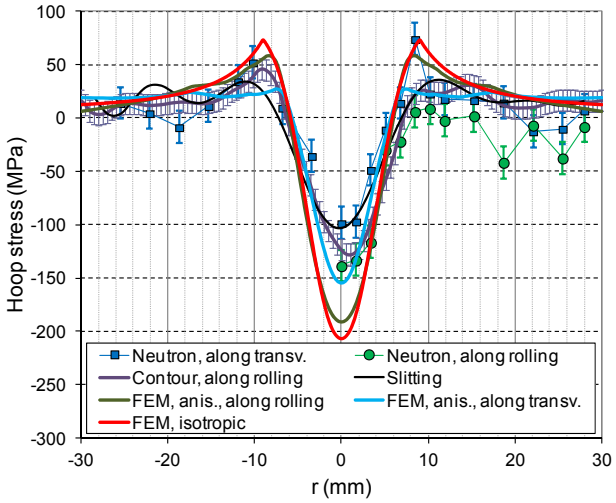

Figure 11 Residual hoop stresses predicted with the anisotropic plasticity model, versus data

Pressure dependent plasticity

In addition to the residual stresses, the simulations were also compared with load-displacement data taken during the indentation process [13]. The displacement portion of the load-displacement data has large uncertainty because of the need to correct for machine compliance and the presence of lubricant during the indentation, but is informative nonetheless. It was hoped that the data was accurate enough to see if the model had larger inaccuracies during the loading or unloading portions of the simulation. Comparing the model prediction to the load-displacement data indicates that the modeled yield strength during loading needs to be about 10% stronger

than what was observed in the uniaxial compression testing in order to match the data. The residual stress results are also consistent with that observation.

Some recent studies have indicated that under conditions of high triaxial compressive stress, such as under the indenters in this experiment, the yield strength in 2024 Al increases [14]. The triaxiality is defined as the ratio of mean stress to effective stress:

$$\eta = \frac{\sigma_m}{\bar{\sigma}} \qquad (1)$$

Figure 12 shows the triaxiality from Eq. 1 plotted at peak load during the simulation. Under the indenter the specimen sees a triaxiality of about -0.8 through the thickness, with peak triaxialities even higher.

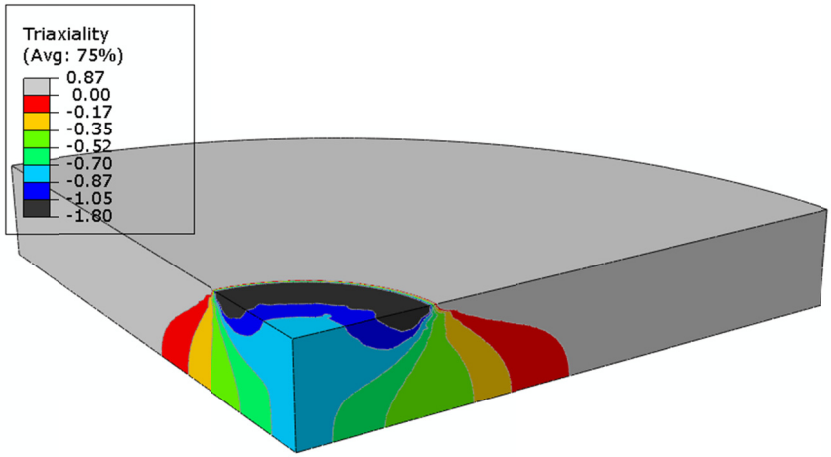

Figure 12 Triaxiality at peak load. The scale zoomed in to show the compressive triaxiality under the indenter

Bai and Wierzbicki [14] give a relation between the yield stress and the triaxiality as

$$\sigma_{yld} = \bar{\sigma}\left(\bar{\varepsilon}_p\right)\left[1 - c_\eta\left(\eta - \eta_0\right)\right] \qquad (2)$$

Where $\bar{\sigma}\left(\bar{\varepsilon}_p\right)$ is the stress-strain curve from the reference test taken at a triaxiality of η_0, which was -1/3 in our uniaxial compression tests. They found a value of c_η of 0.09 for 2024 Al. This would give a strength increase of 4% at a triaxiality of -0.8 and more where the triaxiality is more negative.

The pressure dependent yield strength was implemented into the ABAQUS model by using a user defined field to calculate triaxiality and then augmenting the tabular stress-strain data to provide stresses as a function of the triaxiality to match Eq. 2. Test problems were used to verify that the implementation gave the expected behavior. The Appendix gives the Abaqus input for the constitutive model including the user routine for calculating triaxiality.

The resulting residual stress predictions move the predictions in Figure 10 and Figure 11 in the right direction, but only by about 6 MPa, compared to the 50 MPa that would be needed to match the data.

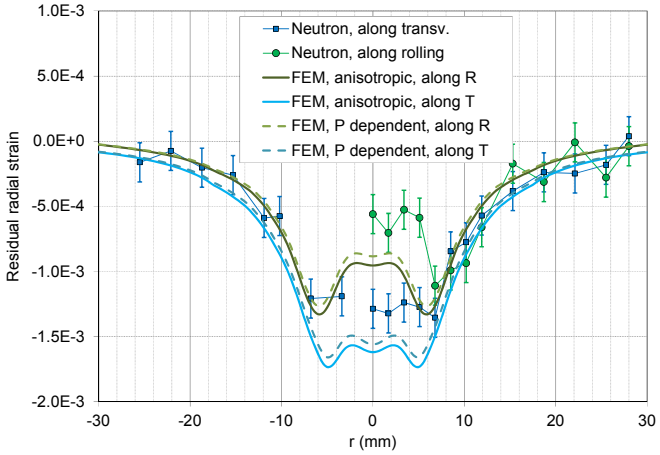

Figure 13 Effect of pressure dependent plasticity model on residual elastic radial strains versus data

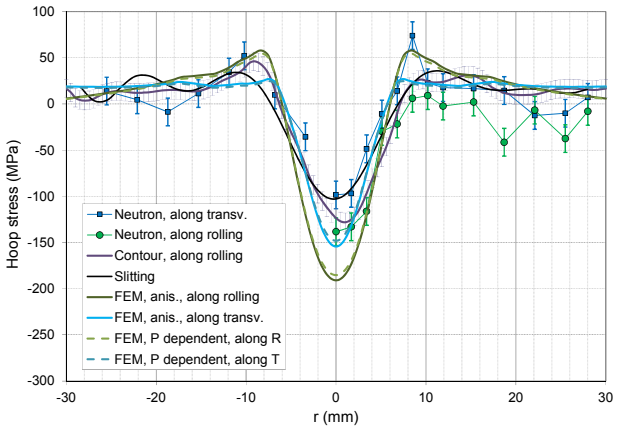

Figure 14 Effect of pressure dependent plasticity model on residual hoop stress versus data

CONCLUSION

The models do not predict the residual stresses in the indented disks as well as hoped. Further studies have shown that the predictions are insensitive to the friction coefficient between the indenter and disk and to other parameters. The most likely explanation remain that the constitutive model is inaccurate in some regard. The next step would be to obtain some *in situ* data during the indentation process. It is hoped that such data would be able to identify if the inaccuracy occurs during the loading or unloading of the indenter, which would narrow down what aspect of the model to improve. The original *in situ* data was load-displacement data on the indenter, but it lacks the necessary sensitivity. The addition of strain gauges to take load-strain data might prove informative.

ACKNOWLEDGEMENTS

This work was performed at Los Alamos National Laboratory, operated by the Los Alamos National Security, LLC for the National Nuclear Security Administration of the U.S. Department of Energy under contract DE-AC52-06NA25396. By acceptance of this article, the publisher recognizes that the U.S. Government retains a nonexclusive, royalty-free license to publish or reproduce the published form of this contribution, or to allow others to do so, for U.S. Government purposes.

REFERENCES

1. Withers PJ (2007) Residual stress and its role in failure. Reports on Progress in Physics 70 (12):2211-2264
2. James MN (2011) Residual stress influences on structural reliability. Engineering Failure Analysis 18 (8):1909-1920
3. Pagliaro P, Prime MB, Clausen B, Lovato ML, Zuccarello B (2009) Known Residual Stress Specimens Using Opposed Indentation. Journal of Engineering Materials and Technology 131:031002
4. Hutchings MT, Withers PJ, Holden TM, Lorentzen T (2005) Introduction to the Characterization of Residual Stress by Neutron Diffraction. Routledge, USA,
5. Woo W, Choo H, Brown DW, Feng Z, Liaw PK (2006) Angular distortion and through-thickness residual stress distribution in the friction-stir processed 6061-T6 aluminum alloy. Materials Science and Engineering: A 437 (1):64-69. doi:10.1016/j.msea.2006.04.066
6. Prime MB, Sebring RJ, Edwards JM, Hughes DJ, Webster PJ (2004) Laser surface-contouring and spline data-smoothing for residual stress measurement. Experimental Mechanics 44 (2):176-184
7. Wilson GS, Grandt Jr AF, Bucci RJ, Schultz RW (2009) Exploiting bulk residual stresses to improve fatigue crack growth performance of structures. International Journal of Fatigue 31 (8-9):1286-1299
8. DeWald AT, Hill MR (2009) Eigenstrain based model for prediction of laser peening residual stresses in arbitrary 3D bodies. Part 1: model description. Journal of Strain Analysis for Engineering Design 44 (1):1-11

9. Cheng W, Finnie I (2007) Residual Stress Measurement and the Slitting Method. Mechanical Engineering Series Springer Science+Business Media, LLC, New York, NY, USA
10. Jones KW, Dunn ML (2008) Fatigue crack growth through a residual stress field introduced by plastic beam bending. Fatigue & Fracture of Engineering Materials & Structures 31 (10):863-875
11. Pagliaro P, Prime MB, Robinson JS, Clausen B, Swenson H, Steinzig M, Zuccarello B (2011) Measuring Inaccessible Residual Stresses Using Multiple Methods and Superposition. Experimental Mechanics 51 (7):1123-1134. doi:10.1007/s11340-010-9424-5
12. Hill R (1948) A Theory of the Yielding and Plastic Flow of Anisotropic Metals. Proceedings of the Royal Society of London Series A Mathematical and Physical Sciences 193 (1033):281-297. doi:10.1098/rspa.1948.0045
13. Pagliaro P (2008) Mapping Multiple Residual Stress Components Using the Contour Method and Superposition. Ph.D. Dissertation, Universitá degli Studi di Palermo, Palermo
14. Bai Y, Wierzbicki T (2008) A new model of metal plasticity and fracture with pressure and Lode dependence. International Journal of Plasticity 24 (6):1071-1096

APPENDIX

For reference, the information to reproduce the constitutive behaviour of this paper is given below in two parts: 1) the information for the input file and 2) the user subroutine for the triaxiality user defined field.

Input file text

```
*USER DEFINED FIELD
*DEPVAR
1
*INITIAL CONDITIONS, TYPE=FIELD, VARIABLE=1
,0
*Material, name=Al2024_cyclic
*Density
 2.7e-09,
*Elastic
73200., 0.33
*Plastic, hardening=isotropic, dependencies=1
80.55, 0.0000e+000, 0.0, -3.000
131.58, 2.5000e-004, 0.0, -3.000
207.90, 5.0000e-004, 0.0, -3.000
252.85, 7.5000e-004, 0.0, -3.000
294.90, 1.0000e-003, 0.0, -3.000
322.78, 1.2500e-003, 0.0, -3.000
341.79, 1.5000e-003, 0.0, -3.000
358.45, 1.7500e-003, 0.0, -3.000
369.07, 2.0000e-003, 0.0, -3.000
377.69, 2.2500e-003, 0.0, -3.000
384.92, 2.5000e-003, 0.0, -3.000
391.61, 2.7500e-003, 0.0, -3.000
397.88, 3.0000e-003, 0.0, -3.000
402.24, 3.2500e-003, 0.0, -3.000
406.36, 3.5000e-003, 0.0, -3.000
410.22, 3.7500e-003, 0.0, -3.000
413.93, 4.0000e-003, 0.0, -3.000
416.46, 4.2500e-003, 0.0, -3.000
419.62, 4.5000e-003, 0.0, -3.000
422.66, 4.7500e-003, 0.0, -3.000
425.34, 5.0000e-003, 0.0, -3.000
```

427.84, 5.2500e-003, 0.0, -3.000
429.73, 5.5000e-003, 0.0, -3.000
432.32, 5.7500e-003, 0.0, -3.000
434.48, 6.0000e-003, 0.0, -3.000
436.50, 6.2500e-003, 0.0, -3.000
438.19, 6.5000e-003, 0.0, -3.000
440.25, 6.7500e-003, 0.0, -3.000
442.01, 7.0000e-003, 0.0, -3.000
443.77, 7.2500e-003, 0.0, -3.000
445.70, 7.5000e-003, 0.0, -3.000
447.06, 7.7500e-003, 0.0, -3.000
448.54, 8.0000e-003, 0.0, -3.000
450.01, 8.2500e-003, 0.0, -3.000
451.31, 8.5000e-003, 0.0, -3.000
452.60, 8.7500e-003, 0.0, -3.000
454.08, 9.0000e-003, 0.0, -3.000
455.52, 9.2500e-003, 0.0, -3.000
457.04, 9.5000e-003, 0.0, -3.000
458.35, 9.7500e-003, 0.0, -3.000
459.51, 1.0000e-002, 0.0, -3.000
461.23, 1.0375e-002, 0.0, -3.000
463.95, 1.0938e-002, 0.0, -3.000
467.77, 1.1781e-002, 0.0, -3.000
472.94, 1.3047e-002, 0.0, -3.000
480.53, 1.4945e-002, 0.0, -3.000
490.26, 1.7793e-002, 0.0, -3.000
503.44, 2.2064e-002, 0.0, -3.000
520.75, 2.8472e-002, 0.0, -3.000
542.84, 3.8083e-002, 0.0, -3.000
562.77, 4.8083e-002, 0.0, -3.000
580.89, 5.8083e-002, 0.0, -3.000
597.08, 6.8083e-002, 0.0, -3.000
611.45, 7.8083e-002, 0.0, -3.000
624.45, 8.8083e-002, 0.0, -3.000
636.16, 9.8083e-002, 0.0, -3.000
646.78, 1.0808e-001, 0.0, -3.000
656.68, 1.1808e-001, 0.0, -3.000
665.60, 1.2808e-001, 0.0, -3.000
673.75, 1.3808e-001, 0.0, -3.000
681.30, 1.4808e-001, 0.0, -3.000
688.23, 1.5808e-001, 0.0, -3.000
694.57, 1.6808e-001, 0.0, -3.000
700.46, 1.7808e-001, 0.0, -3.000
705.87, 1.8808e-001, 0.0, -3.000
710.90, 1.9808e-001, 0.0, -3.000
715.59, 2.0808e-001, 0.0, -3.000
51.32, 0.0000e+000, 0.0, 2.000
83.83, 2.5000e-004, 0.0, 2.000
132.45, 5.0000e-004, 0.0, 2.000
161.09, 7.5000e-004, 0.0, 2.000
187.88, 1.0000e-003, 0.0, 2.000
205.64, 1.2500e-003, 0.0, 2.000
217.75, 1.5000e-003, 0.0, 2.000
228.37, 1.7500e-003, 0.0, 2.000
235.14, 2.0000e-003, 0.0, 2.000
240.62, 2.2500e-003, 0.0, 2.000
245.23, 2.5000e-003, 0.0, 2.000
249.50, 2.7500e-003, 0.0, 2.000

```
253.49, 3.0000e-003, 0.0, 2.000
256.26, 3.2500e-003, 0.0, 2.000
258.89, 3.5000e-003, 0.0, 2.000
261.35, 3.7500e-003, 0.0, 2.000
263.71, 4.0000e-003, 0.0, 2.000
265.33, 4.2500e-003, 0.0, 2.000
267.34, 4.5000e-003, 0.0, 2.000
269.28, 4.7500e-003, 0.0, 2.000
270.99, 5.0000e-003, 0.0, 2.000
272.57, 5.2500e-003, 0.0, 2.000
273.78, 5.5000e-003, 0.0, 2.000
275.43, 5.7500e-003, 0.0, 2.000
276.80, 6.0000e-003, 0.0, 2.000
278.09, 6.2500e-003, 0.0, 2.000
279.17, 6.5000e-003, 0.0, 2.000
280.48, 6.7500e-003, 0.0, 2.000
281.60, 7.0000e-003, 0.0, 2.000
282.72, 7.2500e-003, 0.0, 2.000
283.95, 7.5000e-003, 0.0, 2.000
284.82, 7.7500e-003, 0.0, 2.000
285.77, 8.0000e-003, 0.0, 2.000
286.70, 8.2500e-003, 0.0, 2.000
287.53, 8.5000e-003, 0.0, 2.000
288.35, 8.7500e-003, 0.0, 2.000
289.29, 9.0000e-003, 0.0, 2.000
290.21, 9.2500e-003, 0.0, 2.000
291.18, 9.5000e-003, 0.0, 2.000
292.01, 9.7500e-003, 0.0, 2.000
292.75, 1.0000e-002, 0.0, 2.000
293.85, 1.0375e-002, 0.0, 2.000
295.58, 1.0938e-002, 0.0, 2.000
298.02, 1.1781e-002, 0.0, 2.000
301.31, 1.3047e-002, 0.0, 2.000
306.15, 1.4945e-002, 0.0, 2.000
312.34, 1.7793e-002, 0.0, 2.000
320.74, 2.2064e-002, 0.0, 2.000
331.77, 2.8472e-002, 0.0, 2.000
345.84, 3.8083e-002, 0.0, 2.000
358.54, 4.8083e-002, 0.0, 2.000
370.08, 5.8083e-002, 0.0, 2.000
380.40, 6.8083e-002, 0.0, 2.000
389.55, 7.8083e-002, 0.0, 2.000
397.83, 8.8083e-002, 0.0, 2.000
405.30, 9.8083e-002, 0.0, 2.000
412.06, 1.0808e-001, 0.0, 2.000
418.37, 1.1808e-001, 0.0, 2.000
424.05, 1.2808e-001, 0.0, 2.000
429.24, 1.3808e-001, 0.0, 2.000
434.05, 1.4808e-001, 0.0, 2.000
438.47, 1.5808e-001, 0.0, 2.000
442.51, 1.6808e-001, 0.0, 2.000
446.26, 1.7808e-001, 0.0, 2.000
449.71, 1.8808e-001, 0.0, 2.000
452.91, 1.9808e-001, 0.0, 2.000
455.90, 2.0808e-001, 0.0, 2.000
**
*Potential
 1.162,  1.162,     1.,  1.2364, 1.1, 1.1
```

**

User subroutine to give triaxiality as user defined field

```
      SUBROUTINE USDFLD(FIELD,STATEV,PNEWDT,DIRECT,T,CELENT,
     1 TIME,DTIME,CMNAME,ORNAME,NFIELD,NSTATV,NOEL,NPT,LAYER,
     2 KSPT,KSTEP,KINC,NDI,NSHR,COORD,JMAC,JMATYP,MATLAYO,
     3 LACCFLA)
C
      INCLUDE 'ABA_PARAM.INC'
C
      CHARACTER*80 CMNAME,ORNAME
      CHARACTER*3  FLGRAY(15)
      DIMENSION FIELD(NFIELD),STATEV(NSTATV),DIRECT(3,3),
     1 T(3,3),TIME(2)
      DIMENSION ARRAY(15),JARRAY(15),JMAC(*),JMATYP(*),
     1 COORD(*)
C
C Cet Pressure from stress invariants output
      CALL GETVRM('SINV',ARRAY,JARRAY,FLGRAY,JRCD,JMAC,JMATYP,MATLAYO,LACCFLA)
      PRESS = ARRAY(3)
      SMISES = ARRAY(1)

C Calculate triaxiality
      IF (SMISES .ne. 0) THEN
         TRIAX = -PRESS / SMISES
      ELSE
         TRIAX = 0
      END IF

      FIELD(1) = TRIAX
      STATEV(1) = FIELD(1)
C If error, write comment to .DAT file:
      IF(JRCD.NE.0)THEN
       WRITE(6,*) 'REQUEST ERROR IN USDFLD FOR ELEMENT NUMBER ',
     1     NOEL,'INTEGRATION POINT NUMBER ',NPT
      ENDIF
C
      RETURN
      END
```